CrossMark

# Utilizing the Metallic Nano-Rods in Hexagonal Configuration to Enhance Sensitivity of the Plasmonic Racetrack Resonator in Sensing Application

Mohammad Reza Rakhshani[1] · Mohammad Ali Mansouri-Birjandi[1]

**Abstract** A high sensitive plasmonic refractive index sensor based on metal-insulator-metal (MIM) waveguides with embedding metallic nano-rods in racetrack resonator has been proposed. The refractive index changes of the dielectric material inside the resonator together with temperature changes can be acquired from the detection of the resonance wavelength, based on their linear relationship. With optimum design and considering a tradeoff among detected power, structure size, and sensitivity, the finite difference time domain simulations show that the refractive index and temperature sensitivity values can be obtained as high as 2610 nm per refractive index unit (RIU) and 1.03 nm/°C, respectively. In addition, resonance wavelengths of resonator are obtained experimentally by using the resonant conditions. The effects of nano-rods radius and refractive index of racetrack resonator are studied on the sensing spectra, as well. The proposed structure with such high sensitivity will be useful in optical communications that can provide a new possibility for designing compact and high-performance plasmonic devices.

**Keywords** Surface plasmons · Nanostructures · Optical sensors · Optical resonators

## Introduction

Surface plasmon polaritons (SPPs) are the most effective approach to realize light confinement and manipulation within the nanoscale [1, 2]. Due to the capabilities of overcoming the classical diffraction limit and manipulating light in the nanoscale domain, SPPs have been considered as one of the most promising energy and information carriers [3]. During recent years, a number of plasmonic devices have been proposed such as plasmonic sensor [4], switch [5], and filter [6]. Among these devices, surface plasmon resonance (SPR) sensors are being increasingly studied and attracted considerable attention owing to high value of their sensitivity to the material refractive index and environment temperature, as well as its outstanding performance in miniaturization [7]. In SPR sensors under certain conditions, which are enormously sensitive to the refractive index and the other structural parameters, some resonance modes are excited. In the past, different methods have been proposed for plasmonic sensor such as cavities [8], plasmon-induced transparency (PIT) effects [9], and ring resonators [10]. Ring resonator in a resonant wavelength localizes electromagnetic energy from an input source and only the resonant wavelengths can propagate through the ring resonator fully [11, 12]. Due to their high-quality factor ($Q$), inherent single mode nature, and strong light confinement within a small volume, the optical ring resonators can enhance light–matter interactions and leads to a broad range of applications including refractive index sensing [8].

Metal-insulator-metal (MIM) resonators are especially attractive for the realization of compact sensors due to the strong lateral confinement, but the sensitivity values were not high enough for practical applications. This is principally caused by the low coupling efficiencies arising from the short coupling distance in such structures [13]. Sufficiently, high coupling efficiency is necessary to compensate for the relatively large absorption loss in the plasmonic resonators. Racetrack resonator can offer higher coupling efficiencies owing to its longer coupling region and are more suitable to obtain the desired couplings with respect to ring resonators. In addition,

✉ Mohammad Ali Mansouri-Birjandi
mansouri@ece.usb.ac.ir

[1] Faculty of Electrical and Computer Engineering, University of Sistan and Baluchestan, P. O. Box, Zahedan 98164-161, Iran

🌀 Springer

spacing tolerances are less critical for the coupling gaps in racetracks compared to rings, and it is easier to determine the coupling strength.

Chen et al. researched plasmonic refractive index sensor using rectangular ring MIM waveguide with the sensitivity of 1300 nm/RIU [14]. A plasmonic cavity index sensor based on double metal disks has been established by Kwon in which the value of sensitivity is 1160 nm/RIU [8], while Chen et al. proposed plasmonic sensor based on the MIM ring resonator with same results [15]. To increase the coupling efficiency for plasmonic resonant cavity, we had previously used hexagonal-ring cavity [16]. A plasmonic metal-dielectric-metal (MDM) waveguide structure has been proposed by Wen et al. [17]; they obtained 1131 nm/RIU for refractive index sensitivity. By placing a slot cavity below or above a groove, they designed a plasmonic sensor.

A major limitation of these SPP sensors is due to the lossy nature of their resonance modes, which results from strong absorption of light by the metal nanostructures themselves. As a result, further sensitivity improvements have become increasingly challenging [18]. Plasmonic nano-rods made in different shapes from various metals have attracted researchers' interests significantly. This might be because of their uniqueness in light localization and field enhancement that enables them to have ultra-small mode volumes and enhanced light matter interaction which is vitally desirable for sensing [19]. Hybrid plasmonic–photonic nano-resonators benefit from both the original resonator characteristics and the plasmonic features of the metallic elements. These structural designs provide suitable modal conversion and light coupling conditions. They preserve the characteristics of the original photonic crystal resonators such as a high-quality factor ($Q$) and benefit from the unique features of the metallic element such as the ability to support SPPs and

confine light into ultra-small volumes much beyond its free-space wavelength [20].

In this paper, by using racetrack resonator and embedding the nano-rods, we can reach to a high sensitive sensor. The finite difference time domain (FDTD) method with perfectly matched layer (PML) as boundary conditions is introduced to investigate the transmission and sensing properties of the structure [21]. The remaining parts of the paper are organized as follows. In the "Theory and Model" section, a theory of model is presented and resonance wavelengths are obtained. The "Simulation and Results" section includes simulation results of the structure for verification of the sensitivity. Finally, in the "Conclusion" section, the conclusion will be provided.

## Theory and Model

The proposed sensor structure is schematically shown in Fig. 1, consisting of a racetrack resonator, Ag nano-rods in hexagonal shape, and two waveguides. Racetrack resonators with long lateral interaction length along the entire flat resonator sidewalls are of high importance [22, 23]. Therefore, they can ease the tight constraint on the gap separation between the resonator and the side-coupled waveguide effectively. This feature is an important advantage compared to conventional ring or disk resonators. The material under sensing is filled in the resonator while its refractive index changes caused a shift in wavelength of output channel. We assume the structure is fabricated on the silicon dioxide substrate. The complete set of simulation parameters is summarized in Table 1. Here, the values of $w$, $d$, and $L$ are fixed throughout this paper.



Fig. 1 Schematic of the plasmonic sensor with a racetrack resonator and nano-rods, where $d = 15$ nm, $r = 190$ nm, $L = 40$ nm, $L_c = 120$ nm, $w = 50$ nm, $a = 10$ nm, and $r_{in}/a = 0.5$
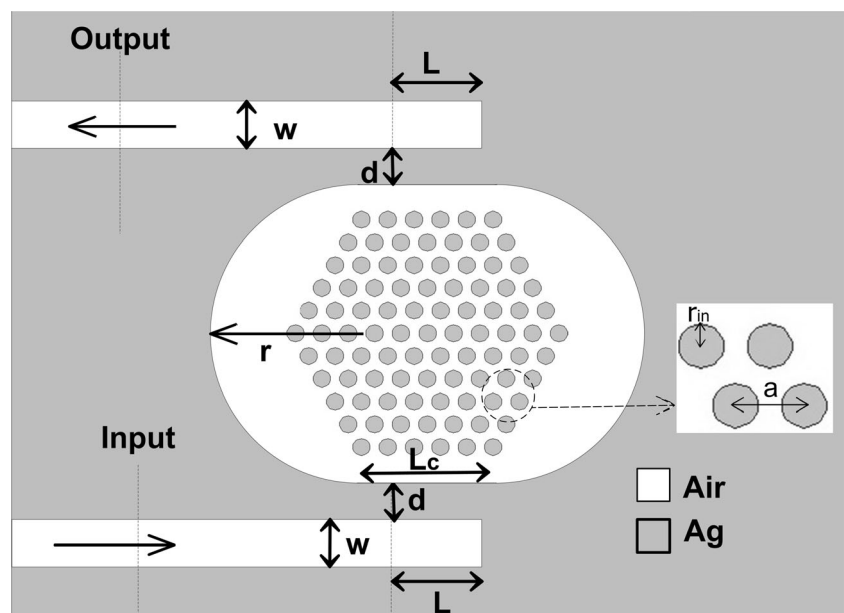
**Table 1** Summary of the simulation model parameters

| Parameter | Symbol | Quantity | Unit |
|-----------|--------|----------|------|
| Waveguide width | $w$ | 50 | nm |
| Coupling length | $L_c$ | 120 | nm |
| Coupling distance | $d$ | 15 | nm |
| Distance between reflector and coupling region | $L$ | 40 | nm |
| Resonator radius | $r$ | 150 | nm |
| Nano-rods' radius | $r_{in}$ | 0.5a | nm |
| Nano-rods' period (lattice constant) | $a$ | 10 | nm |
| Metal thickness | – | 100 | nm |
| Resonator refractive index | $n$ | 1 | – |

We suppose that the medium of the resonator and waveguides is air and its refractive index is 1 ($n = 1$). The background metal and nano-rods are silver, and their permittivity function could be characterized by the Lorentz-Drude model [24, 25]:

$$\varepsilon(\omega) = 1 - \frac{\omega_p^2}{\omega(\omega - i\Gamma_0)} + \sum_{n=1}^{6} \frac{f_n \omega_n^2}{\omega_n^2 - \omega^2 + i\omega\Gamma_n} \tag{1}$$

where $\omega_p$ and $\omega_n$ are indicating the plasma and resonant frequency. As well as, $\Gamma_0$, $\Gamma_n$, and $f_n$ are the damping constant (or collision frequency), damping frequency, and oscillators strength, respectively. We have analytically calculated the permittivity function of silver for different wavelengths by solving Eq. (1), that the numerical values of physical parameters for silver and the permittivity characteristics are given entirely in Ref. [16].

In our simulation, the TM-polarized incident wave with in-plane electric field components is directly coupled to the fundamental SPP mode [26]. When incident optical wave from input source transmits along input waveguide, part of the light is coupled into racetrack resonator, where the forward and backward waves are almost completely reflected in the insulator-metal interfaces. The other part of the light is coupled back into input waveguide. Therefore, standing waves can be formed with some appropriate conditions. Finally, the incident optical wave is converted into two parts, the reflected wave and the transmitted wave, by the resonator. Stable standing waves can only build up constructively within the "resonator" when the following resonant condition is satisfied [27, 28]:

$$\Delta\varphi = m.2\pi \tag{2}$$

here, positive integer $m$ is a positive integer which signifies the resonance order in the resonator. One can get the resonant wavelengths to be [27]

$$\lambda_m = \frac{2n_{eff}S}{m - \frac{\varphi_{ref}}{\pi}} \tag{3}$$

where, $n_{eff}$ is the real part of effective refractive index, $S$ presents the effective length of the resonator, and $\varphi_{ref}$ denotes the phase shift of a beam reflected on insulator-metal interface at each end of the waveguide.

## Simulations and Results

To analyze the properties of the SPP propagation in the structure, the FDTD method is used. The mesh sizes in FDTD simulations are 0.5 nm and the PML as the absorbing boundary condition is used to absorb outgoing waves. Initially, with choosing the resonator refractive index $n = 1$, the output characteristics of the structure has been analyzed. To display the difference, the transmission spectra of the plasmonic sensor with ($r_{in} = 0.5a$) and without ($r_{in} = 0$) the Ag nano-rods are simulated, and the results are shown in Fig. 2. In such conditions, the maximum transmittance occurs at the wavelength of 889 nm and the power transmission for this wavelength is about 73 %. Based on simulation results, in case of having no nano-rods, the corresponding maximum transmittance is 55 %. Therefore, by putting the nano-rods, the transmission efficiency can be improved about 18 %. As shown in Fig. 1, to improve the transmission efficiency, a reflector (with reflective length $L$) was introduced at the right end of the waveguides. The numerical results show that the optimum transmission efficiency is at $L = 40$ nm, in which the peak wavelength is at 889 nm, and the corresponding maximum transmittance is 73 %. By setting $L$, the phase difference of the source and reflected beams can be controlled and strong signal could be obtained by coherent superposition or coherent cancelation condition [29].

As shown in Fig. 3, the impact of output wavelength shift on the transmission spectrum has been studied with increasing racetrack resonator the refractive index $n$ from 1.00 to 1.05 in steps of 0.01, while other parameters are remained unchanged. With the increase of refractive index, the resonance wavelengths exhibit considerable red-shifts. Figure 4 demonstrates approximately a linear relationship between the refractive index of the resonator material and the resonance wavelength, which is very desirable for sensing application and cannot be

**Fig. 2** Normalized transmission spectra of output port without Ag rods (*pink curve*) and with Ag rods (*blue curve*), respectively
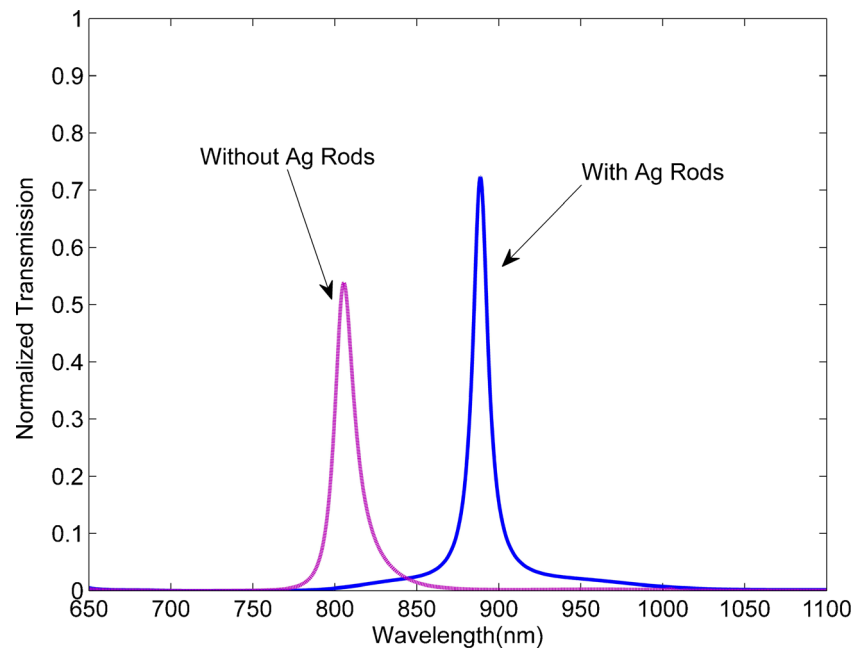


achieved by most other refractive index sensors. Consequently, the refractive index can be obtained easily by certain resonance wavelength based on its linear relationship. The discussions made earlier reveal the properties of sensing performance of our proposed structure as a refractive index sensor. When the refractive index $n$ varies from 1 to 1.05, the shift of resonance wavelength becomes equal to 43 nm. A change in the resonant wavelength $\Delta\lambda$ provides information about the refractive index shift $\Delta n$. To this, it is conventional to define the spectral sensitivity of such sensors as $S = \Delta\lambda/\Delta n$ [30, 31]. All sensors have to be evaluated with respect to their sensitivity [31]. For a plasmonic sensor, its sensitivity ($S$) and figure of merit (FOM) are important parameters to

characterize its performance that the values of these parameters preferred to be much higher. FOM is obtained by dividing the sensitivity by the bandwidth of resonance [full width at half maximum (FWHM)] (FOM = $S/\Delta\lambda_{\mathrm{FWHM}}$) [8]. According to the definition, with $r = 190$ nm, $a = 10$ nm, and $r_{\mathrm{in}}/a = 0.5$ the sensitivity value of plasmonic sensor achieved $S = 860$ nm/RIU which is a high value.

Figure 5a shows the relation between the resonance wavelengths of the sensor and the refractive index of resonator material for different lattice constant $a$. The sensitivity and FOM of proposed structure for different lattice constant $a$ are given in Table 2. As can be observed, by increasing lattice constant $a$ the sensitivity can be increased. An excellent

**Fig. 3** The normalized transmission spectra of the structure for different refractive indices of 1.0~1.05
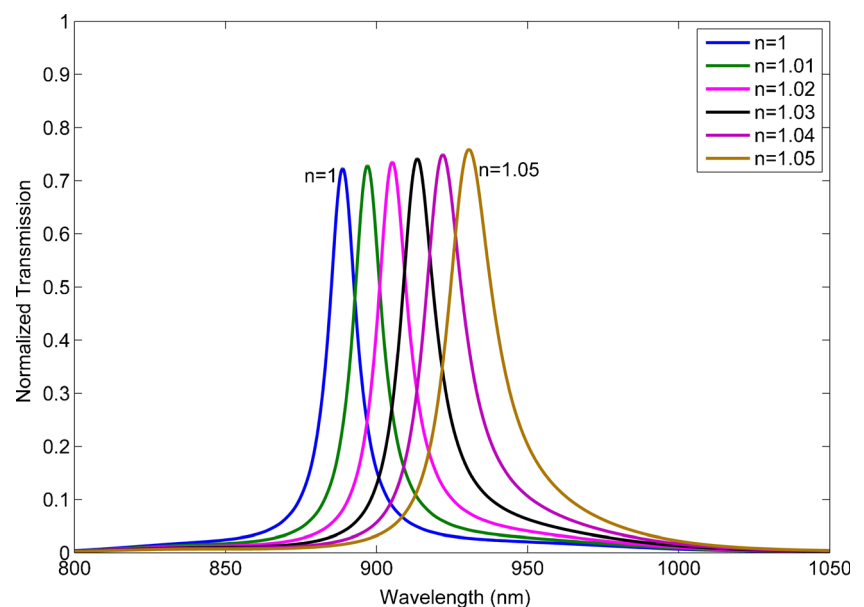
**Fig. 4** Transmitted-peak wavelength of the sensor as a function of refractive index $n$
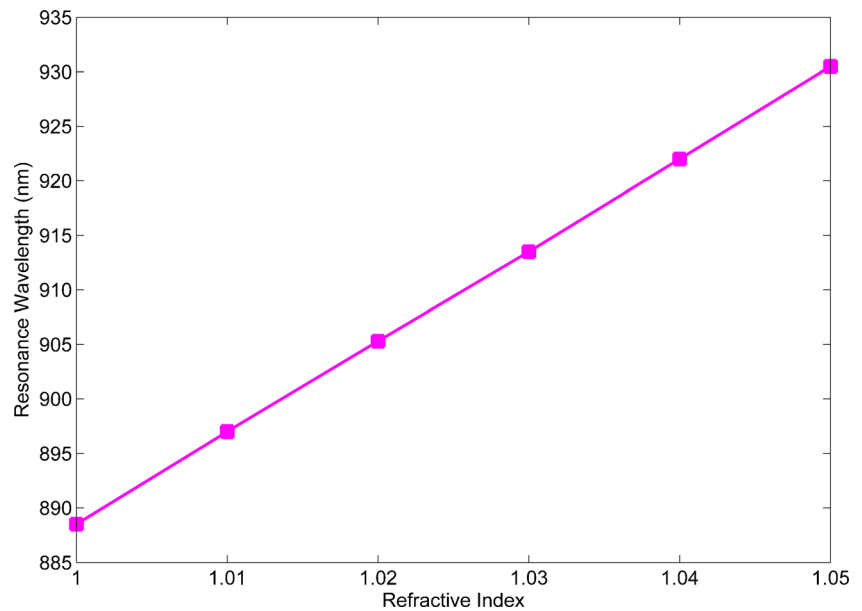
feature of this structure is that there is no need to increase the dimensions of the structure to achieve high sensitivity. In fact, by increasing the Ag nano-rods radius, we can achieve high sensitivities. Figure 5b shows the sensitivity and FOM, wherein, the sensitivity and FOM is almost linear. Through the above analysis, it is obvious that the proposed sensor not only has a high sensitivity but also a relatively high FOM value as well.

Figure 6a illustrates the transmission spectrum of the plasmonic sensor for different refractive indices with $r = 310$ nm, $a = 60$ nm, and $r_{in}/a = 0.5$, while other parameters remained unchanged. The shift in the resonance wavelength when $r$ is set to be 310 $nm$ and the resonator refractive index is varied from 1 to 1.1 becomes equal to 261 nm. Therefore, the sensitivity of the refractive index is as high as 2610 nm/RIU with an FOM of 52 RIU$^{-1}$. As far as we know, this sensitivity value is considerably greater than other reported MIM sensor structures [7, 8, 15, 31–37]. These results demonstrate that the proposed sensor has a high sensitivity value compared to that

of the structure based on a standard ring resonator. The calculated results illustrate that by increasing the radius of the resonator ($r$) the sensitivity can be improved. Nevertheless, the additional transmission loss is also induced with increasing the radius of resonator. On all accounts, we need to make a tradeoff among detected power, structure size, and sensitivity. Therefore, by choosing the value of $r = 310$ nm, $a = 60$ nm, and $r_{in}/a = 0.5$, we have an appropriate sensitivity, structure size, and power transmission values. Magnetic-field pattern at the resonance wavelength of $\lambda = 2.586$ μm is depicted in Fig. 6b. Based on simulation results, in case of having no nano-rods, the corresponding sensitivity is 1240 nm/RIU. Therefore, by putting the nano-rods, the sensitivity can be improved about 1370.

The proposed sensor can also be used for temperature sensing. Temperature sensor is an important device in a wide variety of research applications. As for a temperature sensor, we need to fill the resonator with liquid material that must be sensitive to temperature. In this analysis, we select ethanol
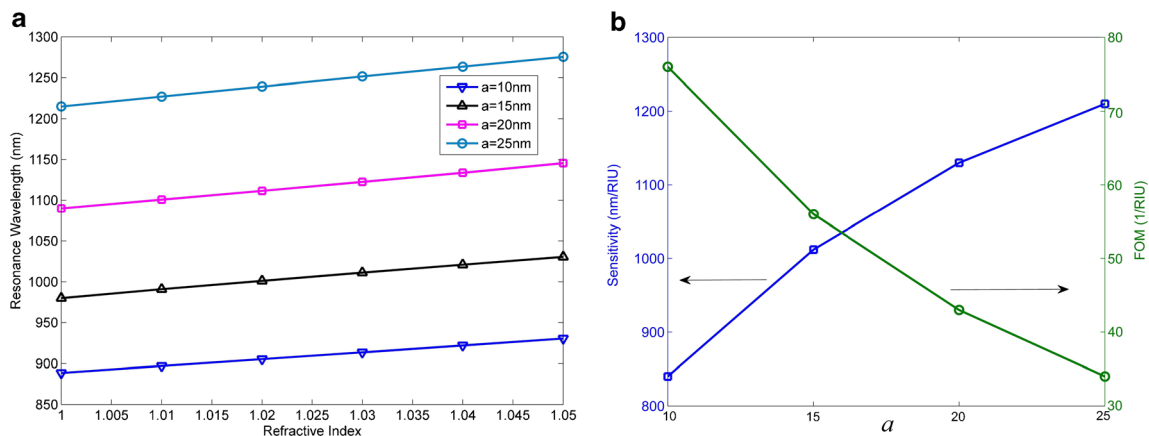


**Fig. 5** **a** The peaks of the transmission spectra versus the different refractive indices for different values of $a$ and $r_{in}$. **b** FOM and sensitivity as a function of $a$

**Table 2** The sensitivity and FOM for different $a$

| $a$ (nm) | Sensitivity (nm/RIU) | FOM (RIU$^{-1}$) |
| --- | --- | --- |
| 10 | 1430 | 37 |
| 15 | 1480 | 34 |
| 20 | 1660 | 32 |
| 25 | 1760 | 30 |

as the sensing material which has a high refractive index-temperature coefficient. The refractive index $n$ related to temperature is evaluated by:

$$n = n_0 + dn/dT(T - T_0) \qquad (4)$$

where $T$ and $n_0$ are the environment temperature and the refractive index of the liquid at the reference temperature $T_0$ (20 °C), respectively, while the values for ethanol are $n_0 = 1.36048$ and $dn/dT = -3.94 \times 10^{-4}$ [36]. From the Eq. (4), it is clear that there is a linear relationship between the temperature of environment and the refractive index of ethanol. The sensitivity of temperature sensor can be defined as $d\lambda/dT$. In order to study the relation between the temperature and the resonance wavelength, we raised the temperature of the medium in intervals of 20 °C from −80 to 78 °C, while the other parameters remained unchanged. Figure 7 illustrates the change of the resonance wavelength by temperature with different values of $a$ and $r_{in}$ in which, when $r = 190$ nm, $a = 25$ nm, and $r_{in}/a = 0.5$ then the shift of the resonance wavelength becomes 86 nm. Consequently, the temperature sensitivity of the sensor can be obtained approximately 0.54 nm/°C. It implies that a linear relation exists between the resonance wavelength and temperature, and the temperature can be obtained by detecting the shift of the resonance wavelength. Also, simulation results show the sensor

Fig. 6 **a** The normalized transmission spectrum for the different refractive indices of the racetrack resonator with $r = 310$ nm, $a = 60$ nm. **b** Magnetic-field pattern of the sensor at resonance wavelength of $\lambda = 2.586$ μm with refractive index $n = 1$
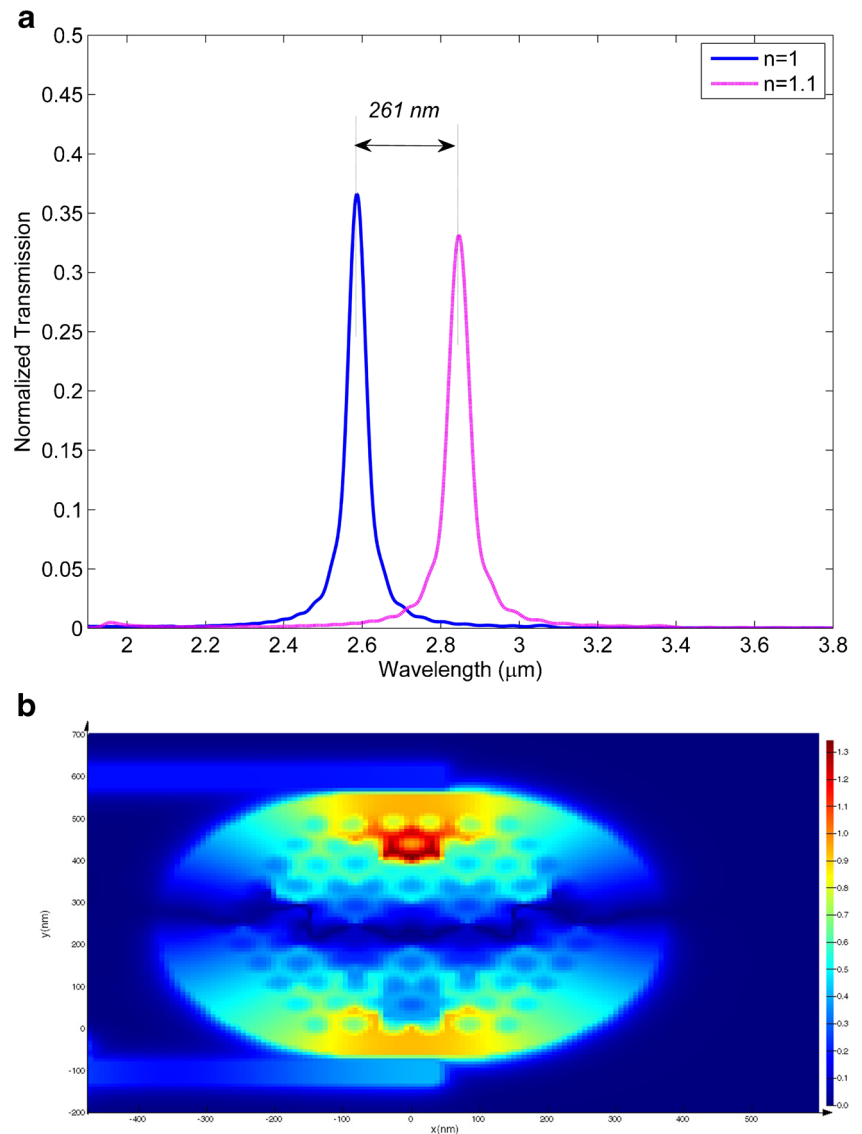
**Fig. 7** The peaks of the transmission spectra versus the different temperature with $r = 310$ nm and different $a$
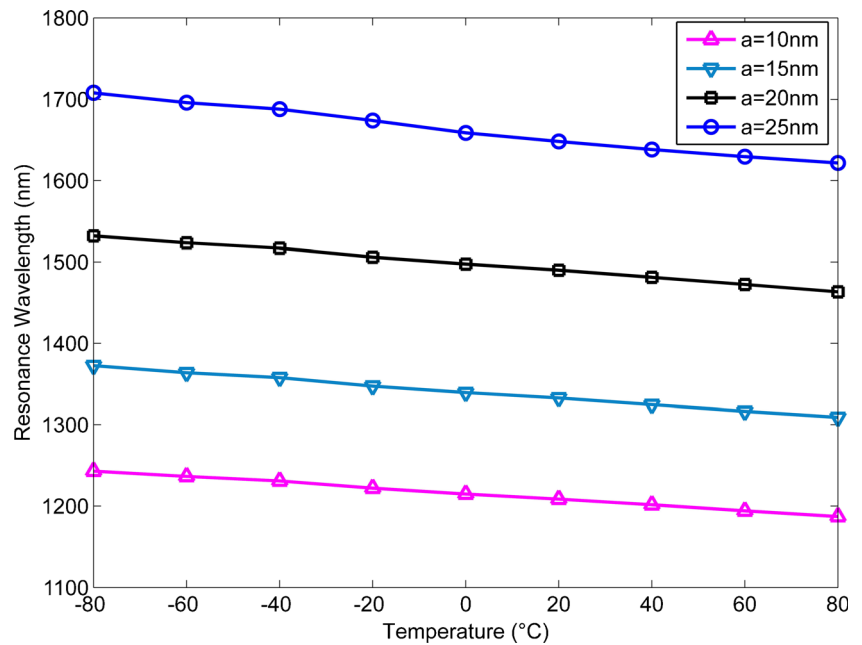


temperature sensitivity can be obtained approximately 1.03 nm/°C for $r = 310$ nm, $a = 60$ nm, and $r_{in}/a = 0.5$. As refractive index of ethanol decreases with the increase of temperature, the resonance wavelength exhibits a blue-shift as a result. The large value of sensitivity achieved in our proposed sensor ($S = 2610$ nm/RIU) opens up the paths for designing real time on-chip optical sensors. Table 3 compares the sensitivity ($S$) for different MIM plasmonic sensors as reported previously.

temperature, and each of them can shift the resonance wavelength linearly alone. We use the racetrack resonator and nano-rods to achieve a highly sensitive and compact plasmonic sensor with the refractive index and temperature sensitivity of 2610 nm/RIU and 1.03 nm/°C, respectively. These results show that the proposed sensor has a high sensitivity value which is nearly two times higher than the sensitivity results reported in the recent papers. The sensor has extensive potential in bio-sensing and optical on-chip nanosensors owing to its high sensitivity, relatively ease fabrication, simple configuration, and compact structure.

## Conclusion

A high sensitive and compact plasmonic refractive index sensor and a temperature sensor using MIM racetrack resonator with nano-rods in hexagonal shape wherein two MIM waveguides coupled to each other by a racetrack resonator filled with under sensing material is proposed and analyzed in this work. The refractive index sensing characteristics of the device are analyzed and simulated by FDTD method and very good linear relationship between the resonance wavelength and the refractive index are obtained. The findings show the increase of the resonator refractive index and/or environment

**Table 3** Sensitivity comparison of different sensor structures

| Reference | Year | Sensitivity (nm/RIU) |
| --- | --- | --- |
| [8, 32, 34] | 2013 | 410~1160 |
| [36] | 2014 | 820 |
| [7, 15, 30, 33, 35] | 2015 | 789~1684 |
| [4, 17, 37] | 2016 | 1131~1820 |
| Our sensor | 2016 | 2610 |

## References

1. Maier SA, Kik PG, Atwater HA, Meltzer S, Harel E, Koel BE, Requicha AA (2003) Local detection of electromagnetic energy transport below the diffraction limit in metal nanoparticle plasmon waveguides. Nature Mater 2(4):229–232
2. Maier SA (2007) Plasmonics: fundamentals and applications. Springer, New York
3. Genet C, Ebbesen TW (2007) Light in tiny holes. Nature 445(7123):39–46
4. Chen Z, Cao X, Song X, Wang L, Yu L (2016) Side-coupled cavity-induced Fano resonance and its application in nanosensor. Plasmonics 11(1):307–313
5. Lu H, Liu X, Wang L, Gong Y, Mao D (2011) Ultrafast all-optical switching in nanoplasmonic waveguide with Kerr nonlinear resonator. Opt Express 19(4):2910–2915
6. Gao Y, Ren G, Zhu B, Huang L, Li H, Yin B, Jian S (2016) Tunable plasmonic filter based on graphene split-ring. Plasmonics 11(1):291–296
7. Li-Ping X, Fa-Qiang W, Rui-Sheng L, Shi-Wei Z, Miao H (2015) A high-sensitivity refractive-index sensor based on plasmonic

waveguides asymmetrically coupled with a nanodisk resonator. Chinese Phys Lett 32(7):070701-1–070701-4

8. Kwon SH (2013) Deep subwavelength-scale metal–insulator–metal plasmonic disk cavities for refractive index sensors. IEEE Photonics Journal 5(1):4800107-1–4800107-7

9. Vafapour Z, Zakery A (2015) New approach of plasmonically induced reflectance in a planar metamaterial for plasmonic sensing applications. Plasmonics 11(2):609–618

10. Wu T, Liu Y, Yu Z, Peng Y, Shu C, Ye H (2014) The sensing characteristics of plasmonic waveguide with a ring resonator. Opt Express 22(7):7669–7677

11. Rakhshani MR, Mansouri-Birjandi MA (2016) Dual wavelength demultiplexer based on metal–insulator–metal plasmonic circular ring resonators. J Mod Opt 63(11):1078–1086

12. Wu YD (2014) High transmission efficiency wavelength division multiplexer based on metal–insulator–metal plasmonic waveguides. J Lightwave Technol 32(24):4242–4246

13. Wang X, Wang P, Chen C, Chen J, Lu Y, Ming H, Zhan Q (2010) Plasmonic racetrack resonator with high extinction ratio under critical coupling condition. J Appl Phys 107(12):124517

14. Chen Z, Cui L, Song X, Yu L, Xiao J (2015) High sensitivity plasmonic sensing based on Fano interference in a rectangular ring waveguide. Opt Commun 340:1–4

15. Chen Z, Yu L, Wang L, Duan G, Zhao Y, Xiao J (2015) Sharp asymmetric line shapes in a plasmonic waveguide system and its application in nanosensor. J Lightwave Technol 33(15):3250–3253

16. Rakhshani MR, Mansouri-Birjandi MA (2016) High sensitivity plasmonic sensor based on metal–insulator–metal waveguide and hexagonal-ring cavity with round-corners. Sensors Journal, IEEE 16(9):3041–3046

17. Wen K, Hu Y, Chen L, Zhou J, Lei L, Meng Z (2016) Single/dual Fano resonance based on plasmonic metal-dielectric-metal waveguide. Plasmonics 11(1):315–321

18. Yu X, Shi L, Han D, Zi J, Braun PV (2010) High quality factor metallodielectric hybrid plasmonic–photonic crystals. Adv Funct Mater 20(12):1910–1916

19. Nezhad MP, Simic A, Bondarenko O, Slutsky B, Mizrahi A, Feng L, Lomakin V, Fainman Y (2010) Room-temperature subwavelength metallo-dielectric lasers. Nat Photonics 4(6):395–399

20. Maksymov IS (2011) Optical switching and logic gates with hybrid plasmonic–photonic crystal nanobeam cavities. Phys Lett A 375(5):918–921

21. Taflove A, Hagness SC (2000) Computational electrodynamics. Artech house publishers

22. Masi M, Orobtchouk R, Fan G, Fedeli JM, Pavesi L (2010) Towards a realistic modelling of ultra-compact racetrack resonators. J Lightwave Technol 28(22):3233–3242

23. Ma N, Li C, Poon AW (2004) Laterally coupled hexagonal micropillar resonator add-drop filters in silicon nitride. Photonics Technology Letters, IEEE 16(11):2487–2489

24. Wang TB, Wen XW, Yin CP, Wang HZ (2009) The transmission characteristics of surface plasmon polaritons in ring resonator. Opt Express 17(26):24096–24101

25. Sulliran DM (1996) Exceeding the courant condition with the FDTD method. IEEE Microw Guided Wave Lett 6(8):289–291

26. Wei PK, Huang YC, Chieng CC, Tseng FG, Fann W (2005) Off-angle illumination induced surface plasmon coupling in subwavelength metallic slits. Opt Express 13(26):10784–10794

27. Zhang Q, Huang XG, Lin XS, Tao J, Jin XP (2009) A subwavelength coupler-type MIM optical filter. Opt Express 17(9):7549–7555

28. Chen L, Liu Y, Yu Z, Wu D, Ma R, Zhang Y, Ye H (2016) Numerical analysis of a near-infrared plasmonic refractive index sensor with high figure of merit based on a fillet cavity. Opt Express 24(9):9975–9983

29. Li Z, Zhang S, Halas NJ, Nordlander P, Xu H (2011) Coherent modulation of propagating plasmons in silver-nanowire-based structures. Small 7(5):593–596

30. Chen S, Meng L, Hu J, Yang Z (2015) Fano interference between higher localized and propagating surface plasmon modes in nanovoid arrays. Plasmonics 10(1):71–76

31. Dolatabady A, Granpayeh N, Nezhad VF (2013) A nanoscale refractive index sensor in two dimensional plasmonic waveguide with nanodisk resonator. Opt Commun 300:265–268

32. Raza S, Toscano G, Jauho AP, Mortensen NA, Wubs M (2013) Refractive-index sensing with ultrathin plasmonic nanotubes. Plasmonics 8(2):193–199

33. Zafar R, Salim M (2015) Enhanced figure of merit in Fano resonance-based plasmonic refractive index sensor. IEEE Sensors J 15(11):6313–6317

34. Ren M, Pan C, Li Q, Cai W, Zhang X, Wu Q, Fan S, Xu J (2013) Isotropic spiral plasmonic metamaterial for sensing large refractive index change. Opt Lett 38(16):3133–3136

35. Xie YY, Huang YX, Zhao WL, Xu WH, He C (2015) A novel plasmonic sensor based on metal–insulator–metal waveguide with side-coupled hexagonal cavity. IEEE Photonics Journal 7(2):1–12

36. Chen Z, Yu L (2014) Multiple Fano resonances based on different waveguide modes in a symmetry breaking plasmonic system. IEEE Photonics Journal 6(6):1–8

37. Binfeng Y, Ruohu Z, Guohua H, Yiping C (2016) Ultra sharp Fano resonances induced by coupling between plasmonic stub and circular cavity resonators. Plasmonics. doi:10.1007/s11468-015-0154-5